Chinese Chemical Letters 31 (2020) 2803–2808

Contents lists available at ScienceDirect

Chinese Chemical Letters

journal homepage: www.elsevier.com/locate/cclet

Communication

# Sustainable activation of peroxymonosulfate by the Mo(IV) in $MoS_2$ for the remediation of aromatic organic pollutants

Mengmeng Du[a,1], Qiuying Yi[a,1], Jiahui Ji[a], Qiaohong Zhu[a], Huan Duan[b], Mingyang Xing[a,*], Jinlong Zhang[a,*]

[a] Key Laboratory for Advanced Materials and Feringa Nobel Prize Scientist Joint Research Center, Key Laboratory for Advanced Materials and Institute of Fine Chemicals, School of Chemistry & Molecular Engineering, East China University of Science & Technology, Shanghai 200237, China
[b] School of Chemistry and Chemical Engineering, Southwest University, Chongqing 400715, China

ARTICLE INFO

*Article history:*
Received 29 May 2020
Received in revised form 13 July 2020
Accepted 4 August 2020
Available online 7 August 2020

*Keywords:*
Peroxymoosulfate
Molybdenum disulfide
Surface reaction
Recyclability
Sulfur vacancies
Density functional theory

ABSTRACT

Although $MoS_2$ has been proved to be a very ideal cocatalyst in advanced oxidation process (AOPs), the activation process of peroxymonosulfate (PMS) is still inseparable from metal ions which inevitably brings the risk of secondary pollution and it is not conducive to large-scale industrial application. In this study, the commercial $MoS_2$, as a durable and efficient catalyst, was used for directly activating PMS to degrade aromatic organic pollutant. The commercial $MoS_2$/PMS catalytic system demonstrated excellent removal efficiency of phenol and the total organic carbon (TOC) residual rate reach to 25%. The degradation rate was significantly reduced if the used $MoS_2$ was directly carried out the next cycle experiment without any post-treatment. Interestingly, the commercial $MoS_2$ after post-treated with $H_2O_2$ can exhibit good stability and recyclability for cyclic degradation of phenol. Furthermore, the mechanism for the activation of PMS had been investigated by density functional theory (DFT) calculation. The renewable $Mo^{4+}$ exposed on the surface of $MoS_2$ was deduced as the primary active site, which realized the direct activation of PMS and avoided secondary pollution. Taking into account the reaction cost and efficient activity, the development of commercial $MoS_2$ catalytic system is expected to be applied in industrial wastewater.



A series of environmental issues, such as air contamination, water pollution, which were caused by the rapid development of industry, have attracted worldwide attention [1–4]. Organic pollutants, especially aromatic compounds containing benzene ring structure, such as phenol, polycyclic aromatic hydrocarbons and other phenols, rhodamine B and other heterocyclic dye molecules, norfloxacin and other antibiotic molecules, are a class of aromatic ring pollutants. Compared with fatty organic pollutants, aromatic ring pollutants are more stable in structure, not easy to decompose, and highly toxic, causing serious pollution to the environment. Recently, many physical methods including absorption and biological treatment have been applied in water treatment [5,6]. However, physical methods can only transfer the aromatic organic pollutant and cannot mineralize the organic molecules, which means it is easy to cause secondary pollution [7–9]. Chemical strategy such as AOPs is a promising approach in water treatment, which can effectively degrade organic pollutions [10,11]. Notably, the reactive oxygen species (ROS) with high standard oxidation potential, such as $^{\bullet}OH$, $SO_4^{\bullet-}$, $O_2^{\bullet-}$, play vital roles in AOPs [12]. For example, the generation of $^{\bullet}OH$ by $H_2O_2$ decomposition has been widely investigated in Fenton or Fenton-like reaction [8,13–15]. However, there remain limitations for the practical application: (1) Ferrous ions can be oxidized into ferric irons, decreasing the ability to decompose $H_2O_2$; (2) low transformation from $Fe^{3+}$ to $Fe^{2+}$ restricts the $^{\bullet}OH$ generation rate; (3) the sensitivity to pH also greatly limits its application in many fields [16–18]. In order to solve these problems, peroxymonosulfate (PMS) has been used to replace $H_2O_2$ in water treatment, generating sulfate radical ($SO_4^{\bullet-}$) [19–21]. Compared with $^{\bullet}OH$, sulfate radicals have higher standard oxidation potential ($SO_4^{\bullet-}$: 2.5–3.1 V; $^{\bullet}OH$: 1.8–2.7 V *vs.* NHE at neutral pH) [22]. Besides, $SO_4^{\bullet-}$ can effectively degrade organic pollutions under a wide pH range (2.0–9.0) [23,24] and possess long half-life (30–40 μs) [25].

Actually, PMS can be activated by different techniques, such as microwave, ultraviolet irradiation, homogeneous/heterogeneous catalysis, heating [26–28]. Nevertheless, homogeneous catalysis

* Corresponding authors.
*E-mail addresses:* mingyangxing@ecust.edu.cn (M. Xing), jlzhang@ecust.edu.cn (J. Zhang).
[1] These authors contributed equally to this work.

https://doi.org/10.1016/j.cclet.2020.08.002
1001-8417/

cannot meet the demand of scalable application owing to the secondary pollution caused by the introduction of transition metal ions in the reaction system [29]. Many researchers have reported that heterogeneous catalysis can effectively active PMS for water treatment. For example, Zhao *et al.* [26] synthesized $CoO_x$-doped mesoporous carbon for activating PMS. As expected, phenol solution could be completely degraded within 60 min in the presence of catalyst and PMS. The structure can affect the catalytic performance [30–32]. Wang *et al.* [16] fabricated variously structured $MnO_2$, such as nanowires, nanorods, and nanotubes, through hydrothermal treatment. Compared with commercial $MnO_2$, those synthesized $MnO_2$ can effectively activate PMS for phenol removing, especially nanowire $MnO_2$ giving an excellent decomposition efficiency of PMS. In our previous work, it was firstly found that the commercial $MoS_2$ could promote the transformation from $Fe^{3+}$ to $Fe^{2+}$ by the exposed $Mo^{4+}$ active sites during the Fenton or Fenton-like reaction [33]. Very recently, Sheng *et al.* [34] successfully employed the $MoS_2/Fe^{2+}$ catalyst to enhance the decomposition efficiency of PMS for the degradation of 2,4,6-trichlorophenol. Subsequently, Wang *et al.* [35] also used $MoS_2$ to promote the activity of $Fe^{2+}$/PMS for the degradation of sulfamethoxazole, which is accelerated by the exposed $Mo^{4+}$ active sites for the improving of $Fe^{2+}/Fe^{3+}$ cycle. Although $MoS_2$ has been proved to be a very ideal cocatalyst in AOPs, the activation process of $H_2O_2$ or PMS is still inseparable from metal ions such as $Fe^{2+}$, $Co^{2+}$, which inevitably brings the risk of secondary pollution such as iron sludge formation, and it is not conducive to large-scale industrial application. There is thereby an urgent need but it is still a significant challenge to develop an inorganic catalyst with durable and efficient activity to directly activate PMS without the need for free metal ions.

Herein, we found that the commercial $MoS_2$ (Micron size) can directly activate PMS with a durable and efficient activity for the degradation of aromatic organic pollutants including phenol, dyes and antibiotics. The influence of parameters including pH value, dosage of PMS and $MoS_2$ on the remediation of organic pollutants were also investigated. It was noteworthy that 10 mg/L phenol could be efficiently degraded within 25 min with low amount of PMS (0.5 mmol/L), and $MoS_2$ exhibited good stability after cyclic degradation of phenol, which was much better than most reported heterogeneous catalytic PMS activation, such as recognized high efficiency Co/PMS system. Moreover, the mechanism for the activation of PMS over $MoS_2$ had been investigated by the combination of experiment and DFT calculation.

The reagents and experimental procedures are present in Supporting information. X-ray diffraction (XRD) patterns of all samples were collected in the range 5°-80° ($2\theta$) using a Rigaku D/MAX 2550 diffractometer (Cu K$\alpha$ radiation, $\lambda$ = 1.5406 Å), operated at 40 kV and 100 mA. The morphologies were characterized by transmission electron microscopy (TEM, TEM1400). The instrument employed for X-ray photoelectron spectroscopy (XPS) studies was a Perkin-Elmer PHI 5000C ESCA system with Al K$\alpha$ radiation operated at 250 W. The shift of the binding energy due to relative surface charging was corrected using the C 1s level at 284.6 eV as an internal standard. The electron paramagnetic resonance (EPR) were recorded at room temperature using Varian E-112. Raman measurements were performed at room temperature by using Raman microscopes (Renishaw, U. K.) under the excitation wavelength of 532 nm. The dissolution of $MoS_2$ were measured by the inductively coupled plasma optical emission spectrometry (ICP-OES, Perkin-Elmer Optima 7300DV ICP-OES apparatus combined an SCD detector and an echelle optical system). The total organic carbon (TOC) concentration of the degradation agent was recorded using a SHIMADZU TOC-L CPN analyzer. Besides, the density functional theory (DFT) calculations are present in Supporting information.

In order to evaluate the roles of commercial $MoS_2$ on PMS activation, phenol degradation experiments were carried out. As shown in Fig. 1a, it can be seen that the content of phenol was unchanged in the presence of $MoS_2$ alone, indicating that the adsorption of organic matter by the catalyst is basically negligible. In the presence of PMS alone, 10% phenol could be degraded. Those results illustrate that phenol cannot be efficiently oxidized in the presence of commercial $MoS_2$ alone or PMS alone. As expected, in the presence of commercial $MoS_2$ and PMS, the removal efficiency of phenol was obviously improved, which can degrade 80% phenol within 25 min, indicating that commercial $MoS_2$ can significantly enhance the activation of PMS, thereby generating more reactive species for phenol degradation.

Zero order reaction model was used to describe its kinetics: $C_0 - C = kt$, where $C$ (mg/L) means the phenol concentration at a reaction time ($t$, min), and $C_0$ (mg/L) means the initial concentration of phenol, and $k$ (mg $L^{-1}$ $min^{-1}$) is the zero order kinetic constant [36]. As illustrated in Fig. 1b, the kinetic constant with only PMS (0.007 mg $L^{-1}$ $min^{-1}$) added is much lower than that in the $MoS_2$/PMS system (0.196 mg $L^{-1}$ $min^{-1}$). Therefore, the presence of the catalyst can promote more efficient activation of PMS. However, many factors such as PMS dosage, $MoS_2$ dosage and pH value would influence the performance of $MoS_2$/PMS process, which were discussed in supporting information (Fig. S1 in Supporting information). Besides, the catalytic activity under different initial phenol concentration was carried out. There was no doubt that the degradation rate would decrease with the increasing of initial phenol concentration. The catalytic activity

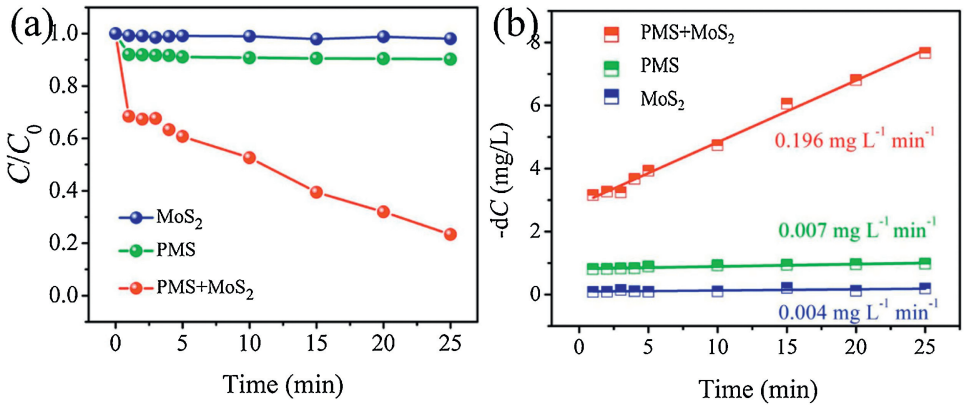


**Fig. 1.** (a) Phenol removing under different condition, condition: [PMS] = 0.5 mmol/L, catalyst = 0.8 g/L, $[Phenol]_0$ = 10 mg/L, T = 298 K, initial pH 3.0; (b) the corresponding kinetic constants.

dropped when the initial phenol concentration adding from 10 mg/L to 30 mg/L (Fig. S2 in Supporting information).

The mineralization of phenol under neutral condition by $MoS_2$/PMS process was present in Fig. 2a. Approximately 25% of TOC was removed. After regularly adding 0.5 mmol/L PMS at a time of 30 min, the TOC was degraded from 75% to 25%, which demonstrates that the increase of PMS dose can greatly enhance the mineralization rate during the degradation process. In other words, $MoS_2$ can continuously decompose PMS and achieve deep degradation of aromatic organic pollutants. The $MoS_2$/PMS system for phenol degradation can extend to remove other aromatic organic pollutants including Congo red (CR), methylene blue (MB), sulfadiazine (SD), norfloxacin (NOR), enrofloxacin (ENR) and bisphenol A (BPA) (Fig. 2b and Fig. S3 in Supporting information). Seen from Fig. S3, compared with pure PMS system, the activity of degradation of various organic pollutants in $MoS_2$/PMS system was significantly improved. Pure PMS had limited activity in degrading organic pollutants (degradation rates: 23% ~ 63%), adding $MoS_2$ could improve the decomposition efficiency of PMS, and achieve deep degradation of most organic pollutants within 30 min (degradation rates: > 98%). The above results indicated that $MoS_2$/PMS involved AOPs is expected to achieve the complex wastewater treatment. In addition, the $MoS_2$/PMS system has been compared with other recently reported heterogeneous catalyst systems (the last three years of coverage), as shown in Table S1 (Supporting information). Most reported catalysts require relatively high concentrations of PMS (1 ~ 5 mmol/L) and take a long time (60 ~ 700 min) to achieve a removal rate of organic pollutants over 90% [37–48].

The stability of catalyst is a critical property for practical applications. Evidences, such as XRD (Fig. 2c) and TEM (Fig. S4 in Supporting information) could prove the stability of catalyst. The crystal and morphology of $MoS_2$ did not change significantly after the reaction. Cycling runs were performed under the same condition as shown in Fig. 2d. About 85% phenol can be degraded within 30 min. After the reaction, the degradation rate of phenol was significantly reduced if the used $MoS_2$ was directly carried out the next cycle experiment without any post-treatment. Interestingly, if the used $MoS_2$ was post-treated with $H_2O_2$, the efficiency of the cyclic reaction was significantly improved. XRD pattern after post-treated with $H_2O_2$ was shown in Fig. S5 (Supporting information). The efficiency had a negligible decrease after five cycles, and the results demonstrated that commercial $MoS_2$ had good durability and recyclability for the activation of PMS. Our previous work has demonstrated that $H_2O_2$ can react with $Mo^{6+}$ exposed on the surface of $MoS_2$ to regenerate the highly reductive active site of $Mo^{4+}$ [33]. The circulation of $Mo^{6+}/Mo^{4+}$ on $MoS_2$ surface is the key to ensure its recyclable and effective activation of PMS (Eq. 1). Moreover, after three cycles, the activity of many reported catalytic systems decreased to varying degrees. In general, compared with various reported efficient heterogeneous catalytic PMS systems, $MoS_2$/PMS system has significant advantages in both degradation rate of organic pollutants and the stability of catalyst. It is worth mentioning that in most reaction systems with high activity, the synthesis of catalysts is relatively complex and costly, while the catalyst we used here is commercial $MoS_2$, with relatively low cost.

$$\text{Interface: } Mo^{6+} + H_2O_2 \rightarrow Mo^{4+} + O_2 + 2H^+ \quad (1)$$

In order to determine the radical species in reaction process, tert-butyl alcohol (TBA) and methanol (MeOH) were used as scavengers for scavenging experiments to verify the active intermediates (Fig. 3a). Noting that TBA is easier to react with $^{\bullet}OH$ compared to $SO_4^{\bullet-}$ ($k_{\cdot OH} = 6.0 \times 10^8$ L mol$^{-1}$ s$^{-1}$), while methanol reacts with both $^{\bullet}OH$ and $SO_4^{\bullet-}$ ($k_{\cdot OH} = 9.7 \times 10^8$ L mol$^{-1}$ s$^{-1}$ and $k_{SO_4^{\bullet-}} = 2.5 \times 10^7$ L mol$^{-1}$ s$^{-1}$) [49,50]. As depicted in Fig. 3a, the phenol degradation rate can reach up to 80% without quenching agents. When TBA was added into reaction solution, the

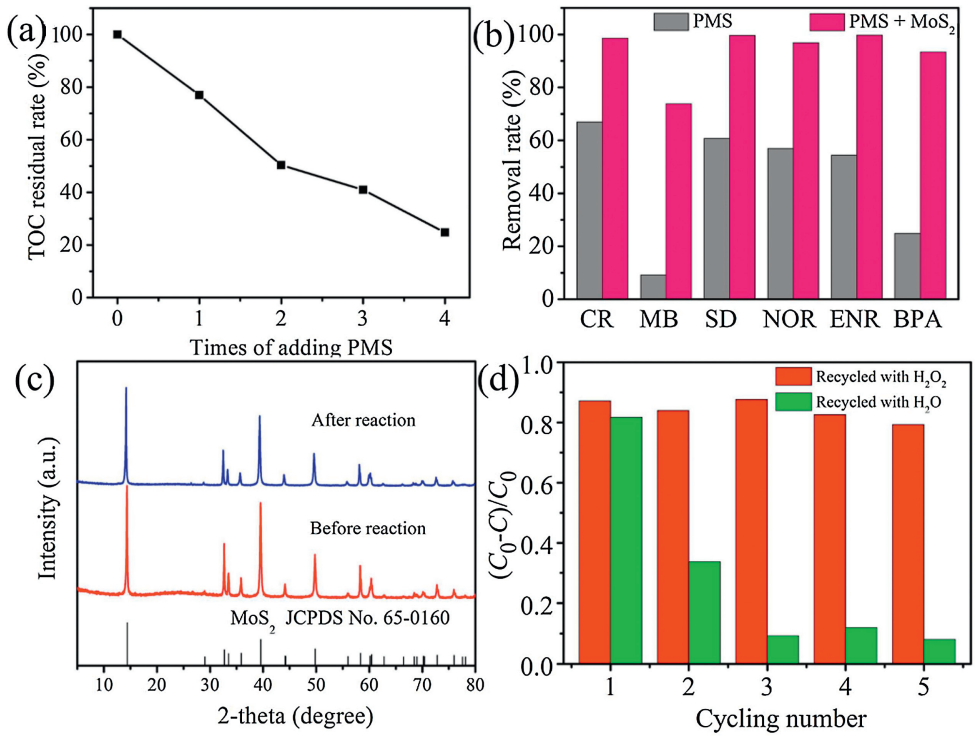


**Fig. 2.** (a) TOC removal tests under $MoS_2$/PMS system (condition: catalyst = 0.8 g/L, $[Phenol]_0$ = 10 mg/L, T = 298 K, initial pH 7.0; regularly adding 0.5 mmol/L PMS at a time of 30 min); (b) Removal efficiency of various organic pollutants including phenol, dyes and antibiotics. Reaction conditions: [CR] = 20 mg/L, [MB] = 20 mg/L, [SD] = 10 mg/L, [NOR] = 10 mg/L, [ENR] = 10 mg/L, [BPA] = 10 mg/L, [PMS] = 0.5 mmol/L, catalyst = 0.8 g/L, T = 298 K, initial pH 7.0. (c) XRD patterns of $MoS_2$ before and after reaction. (d) Cycling experiment on removal of phenol.

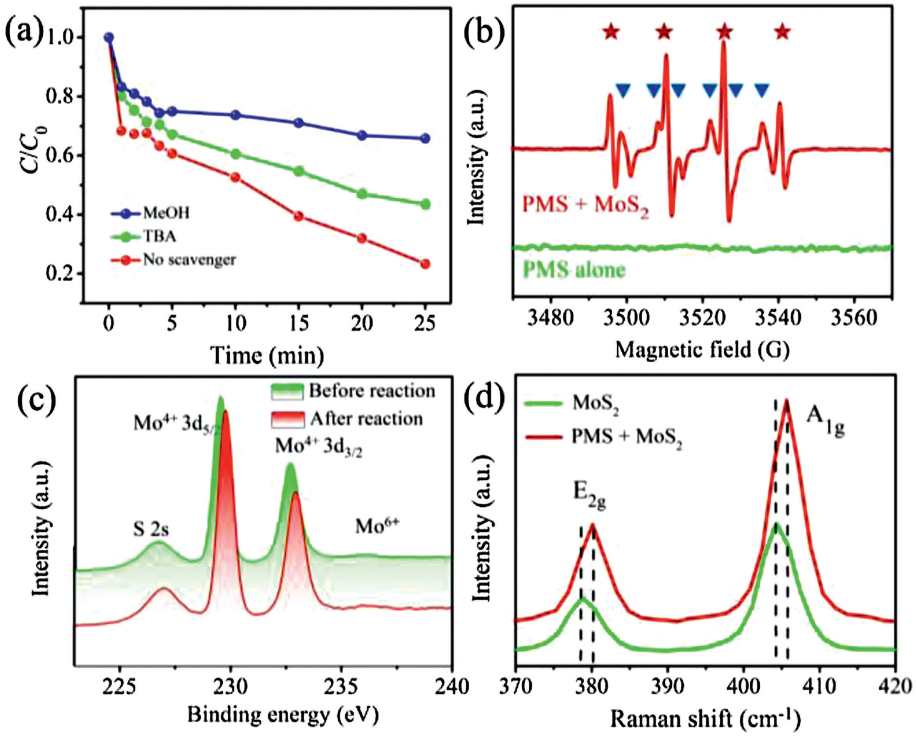


**Fig. 3.** (a) Quenching test on phenol degradation using TBA and MeOH (condition: catalyst = 0.8 g/L, $[Phenol]_0$ = 10 mg/L, [PMS] = 0.5 mmol/L, [TBA] = 0.1 mmol/L, [MeOH] = 0.1 mmol/L, T = 298 K, initial pH 7.0). (b)EPR spectra obtained from the pure PMS and $MoS_2$/PMS systems with DMPO as a spin-trapping reagent (★ represents DMPO−OH adduct and ▼ represents DMPO-$SO_4$ adduct). (c) Mo 3d XPS spectra of $MoS_2$ before and after reaction. (d) Raman spectra of $MoS_2$ before and after reaction.

decrease of removal efficiency suggests that the solutions contains $^{\bullet}OH$. However, the degradation rate of phenol was lower than the rate of TBA as quenching agent when methanol was added as the scavenge agent, indicating that $SO_4^{\bullet-}$ also exist in solution. As shown in Fig. 3b, no characteristic signal was observed in solution containing 5,5-dimethyl-1-pyrroline (DMPO) and PMS. Both hydroxyl radicals and sulfate radicals can detected in PMS/$MoS_2$ system. The peaks with the intensity ratio of 1:2:2:1 (special hyperfine coupling constants $\alpha N = \alpha H = 14.9$ G) can belong to DMPO−OH, and the character peaks of DMPO-$SO_4$ can be observed around DMPO−OH. Besides, the enhanced signal changing when 2,2,6,6-tetramethylpiperidine (TEMP) as trapping reagent indicates that singlet oxygen also exists in the system (Fig. S6 in Supporting information). Those results show that $^{\bullet}OH$, $SO_4^{\bullet-}$ and $^1O_2$ were the radical species in phenol degradation.

The chemical bonding environment of Mo atom was characterized by XPS. In Fig. 3c, the peaks of Mo 3d at 232.7 eV and 229.6 eV belong to $Mo^{4+}$ $3d_{5/2}$ and $Mo^{4+}$ $3d_{3/2}$, respectively. And the binding energy of 226.8 eV is assigned to S 2 s peak [51]. All peaks in XPS spectrum of Mo element after reaction moved to higher binding energy, such as the $3d_{3/2}$ peak moved from 229.6 eV to 229.8 eV and the $3d_{5/2}$ peak migrated from 232.7 eV to 233.0 eV, which indicates the electron density around Mo decreased. As described in Eq. 2, the electrons from Mo to PMS are the key to form $SO_4^{\bullet-}$. Besides, $^{\bullet}OH$ can generate from $SO_4^{\bullet-}$. Interesting, the peak intensity of $Mo^{6+}$ has barely increased after reaction, which can be ascribed to that the $Mo^{6+}$ can be reduced by $HSO_5$- to regenerate $Mo^{4+}$(Eq. 3). Raman spectra confirm that the surface Mo element has been oxidized. As seen in Fig. 3d, the character peak of $A_{1g}$ at 405.87 $cm^{-1}$ is slightly blue-shift compared to the $MoS_2$ before reaction (1.6 $cm^{-1}$), suggesting electron-phonon interaction changed [51]. It is easy to understand the phenomenon that the commercial $MoS_2$ contains many defects as active centers (Fig. S7 in Supporting information), and the surface electrons flow to PMS during activation and then form radical species to degrade pollutants (Eq. 4). The oxidation of phenol can suppose as follows. The formed radical species attack the phenol molecule to form some intermediate products such as some carboxylic acid compounds. With the further oxidation, those compounds can be further oxidized into $CO_2$ and $H_2O$. Our previous work has demonstrated that the sulfur defects can provide reduction active sites on the surface of $MoS_2$ by the exposing of $Mo^{4+}$ [33].

$$\text{Interface: } Mo^{4+} + HSO_5^- \rightarrow Mo^{6+} + SO_4^{\bullet-} + OH^- \quad (2)$$

$$\text{Interface: } Mo^{6+} + HSO_5^- \rightarrow Mo^{4+} + SO_5^{\bullet-} + H^+ \quad (3)$$

$$\text{Solution: } {}^{\bullet}OH/SO_4^{\bullet-} + \text{phenol} \rightarrow \text{intermediates} + H_2O + CO_2 \quad (4)$$

In addition to explore the mechanism of activation of PMS by $MoS_2$, more supporting experiments were carried out. First, the dissolved amount of molybdenum ions are around 1%. Previous literature reported that metal ions could effectively active PMS for pollution degradation [52,53]. Therefore, it is necessary to verify the effect of the dissolved molybdenum ions on PMS activation (Fig. S8 in Supporting information). The result demonstrates 18% phenol can be degraded in the system by the dissolved metal ion and PMS, meaning the degradation efficiency of homogeneous catalysis cannot be ignored. This result shows that the dissolved Mo ions also have a certain ability to activate PMS. Although both homogeneous and heterogeneous catalysis exists in the system, the efficiency of homogeneous catalysis is far lower than heterogeneous catalysis. The dissolved Mo ion can be removed by flocculation and used iron ions as flocculant, the final residual dissolution rate of Mo ion was reduced to 0.16% (Table S2 in

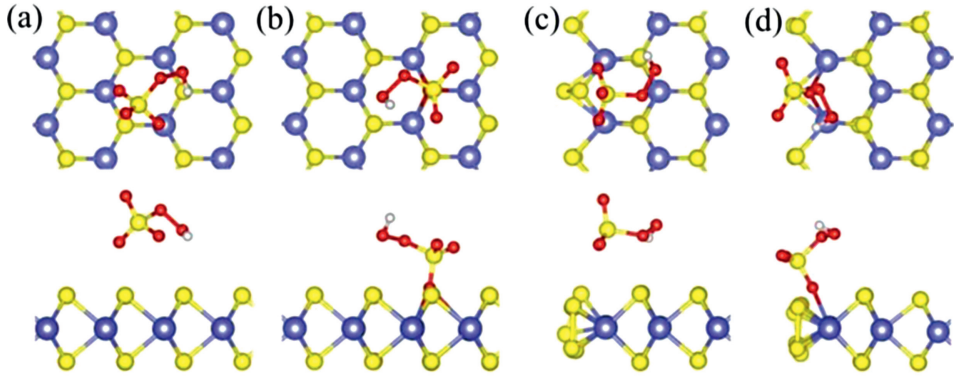


**Fig. 4.** The optimal adsorption configuration of PMS molecules on the basal plane and zigzag edge of 2H-$MoS_2$ nanosheet, respectively. Both the top view (up) and side view (down) were presented here. (a) PMS on the basal plane, (b) PMS on the basal plane with $V_S$, (c) PMS on the zigzag edge, (d) PMS on the zigzag edge with $V_S$. The blue, red, yellow, and white atoms are Mo, O, S, and H atoms, respectively.

Supporting information). To investigate the influence of sulfide ions, $Na_2S$ was employed as sulfur source to active PMS (Fig. S9 in Supporting information). Less than 5% phenol can be degraded indicating sulfide ions cannot active PMS. Based on the above results, it can be concluded that the exposed $Mo^{4+}$ on $MoS_2$ surface rather than the dissolved molybdenum ions or sulfide ions was the main active site for the activation of PMS.

To reveal the effect of $MoS_2$ nanosheet with sulfur vacancies (labeled as $V_S$) on the catalytic properties of PMS molecules, the potential bonding site, adsorption energy, and electron transfer of the activation process had been examined for capturing the essential characteristics of nonradical oxidation [54]. Firstly, we carried out the DFT calculations to acquire the possible adsorption configurations of PMS molecules on 2H-$MoS_2$ basal plane and zigzag edge sites (Fig. 4 and Table S3 in Supporting information). The formation energies of these two structures were −0.53 and −0.71 eV, respectively. To some degree, they were slighter than that of $H_2O_2$ molecules, which formed two distorted hydrogen bonds. From Fig. 4 and Table S3, the adsorption of PMS molecules on the $MoS_2$ without discontinuity was quite minor due to the weak physical interaction, a few electrons transferred between them, and the bond length of $[SO_4–OH]^-$ was stretched after adsorption. However, if the $V_S$ were abundant in the $MoS_2$ basal plane or zigzag edge sites (Fig. 4), the PMS molecule adsorption enhanced greatly, which implied that the bonding between PMS with the bare Mo atoms was thermodynamically favorable, the adsorption energy increased by almost 2 times, the charge transfer increased 3 times more, and the O—O bond length was further prolonged (Table S3). Therefore, the presence of $V_S$ could facilitate the adsorption capability of PMS, activate the molecules *via* forming Mo-O bond for electron transfer from $MoS_2$ nanosheet to PMS. Furthermore, the asymmetric structure of PMS ($HSO_5^-$) and the enhanced adsorption and oxidation ability on the defective $MoS_2$ sheet might contribute to the proposed nonradical reaction to form radical species.

In conclusions, economic $MoS_2$ can efficiently activate PMS to generate radical species, like $^{\bullet}OH$, $SO_4^{\bullet-}$ and $^1O_2$, which have high oxidation potential for the remediation of organic pollutants. The kinetic constant of the commercial $MoS_2$ activating PMS is 28 times than pure PMS. And PMS could be activated at a wide range of pH value especially at neutral condition. Moreover, 75% TOC could be removed in $MoS_2$/PMS system. Besides, this $MoS_2$/PMS system can effectively remove various organic pollutants including phenol, dyes and antibiotics within short time. Importantly, phenol can be degraded continuously by the commercial $MoS_2$ after post-treated with $H_2O_2$ with good stability and recyclability, thus solving the devitalization of traditional catalyst. DFT calculation reveals that the sulfur defect can improve the adsorption of PMS on the surface of $MoS_2$, thus the O—O bond length is further prolonged to form radicals species. Besides, $MoS_2$ is the main component of molybdenite, and molybdenite is the most widely distributed molybdenum mineral with real industrial value among more than 30 molybdenum minerals known in nature. The development of commercial $MoS_2$ catalytic system for efficient activation of PMS is expected to reduce reaction cost and be used for large-scale treatment of industrial waste water.

## Declaration of competing interest

The authors declare no competing financial interest.

## Acknowledgments

This work was supported by the State Key Research Development Program of China (No. 2016YFA0204200). Project supported by Shanghai Municipal Science and Technology Major Project (No. 2018SHZDZX03) and the Program of Introducing Talents of Discipline to Universities (No. B16017). National Natural Science Foundation of China (Nos. 21822603, 21811540394, 5171101651, 21677048, 21773062, 21577036), and the Fundamental Research Funds for the Central Universities (No. 22A201514021). The authors thank to Research Center of Analysis and Test of East China University of Science and Technology for the help on the characterization.

## Appendix A. Supplementary data

Supplementary material related to this article can be found, in the online version, at doi:https://doi.org/10.1016/j.cclet.2020.08.002.

## References

[1] P. Liang, C. Zhang, X. Duan, et al., Environ. Sci. Nano 4 (2017) 315–324.
[2] M. Du, B. Qiu, Q. Zhu, M. Xing, J. Zhang, Catal. Today 327 (2019) 340–346.
[3] P. Du, R. Eisenberg, Energy Environ. Sci. 5 (2012) 6012–6021.
[4] C. Dong, C. Lian, S. Hu, et al., Nat. Commun. 9 (2018) 1252.
[5] Z. Zhu, L. Zhong, Z. Zhang, et al., J. Mater. Chem. A 5 (2017) 25266–25275.
[6] D. Jonckheere, J.A. Steele, B. Claes, et al., ACS Appl. Mater. Interfaces 9 (2017) 30064–30073.
[7] M. Xing, W. Xu, C. Dong, et al., Chem 4 (2018) 1359–1372.
[8] C. Dong, J. Lu, B. Qiu, et al., Appl. Catal. B: Environ. 222 (2018) 146–156.
[9] G. Zhu, S. Wang, Z. Yu, et al., Res. Chem. Intermed. 45 (2019) 3777–3793.
[10] H. Zhang, Q. Ji, L. Lai, G. Yao, B. Lai, Chin. Chem. Lett. 30 (2019) 1129–1132.
[11] J. Li, Y. Li, Z. Xiong, G. Yao, B. Lai, Chin. Chem. Lett. 30 (2019) 2139–2146.
[12] A. Khan, H. Wang, Y. Liu, et al., J. Mater. Chem. A 6 (2018) 1590–1600.

[13] B. Qiu, Y. Deng, M. Du, M. Xing, J. Zhang, Sci. Rep. 6 (2016) 29099.
[14] H. Zhong, L. Duan, P. Ye, et al., Res. Chem. Intermed. 45 (2019) 907–918.
[15] Q. Yi, J. Ji, B. Shen, et al., Environ. Sci. Technol. 53 (2019) 9725–9733.
[16] Y. Wang, S. Indrawirawan, X. Duan, et al., Chem. Eng. J. 266 (2015) 12–20.
[17] H. Zhang, X. Liu, J. Ma, et al., J. Hazard. Mater. 344 (2018) 1220–1228.
[18] B. Qiu, M. Xing, J. Zhang, J. Mater. Chem. A 3 (2015) 12820–12827.
[19] J. Zou, J. Ma, L. Chen, et al., Environ. Sci. Technol. 47 (2013) 11685–11691.
[20] Q. Yi, W. Liu, J. Tan, et al., Chemosphere 244 (2020) 125539.
[21] J. Ji, R.M. Aleisa, H. Duan, et al., iScience 23 (2020) 100861.
[22] R. Yuan, L. Hu, P. Yu, et al., Chemosphere 198 (2018) 204–215.
[23] H. Li, C. Shan, B. Pan, Environ. Sci. Technol. 52 (2018) 2197–2205.
[24] J. Zou, J. Ma, L. Chen, et al., Environ. Sci. Technol. 47 (2013) 11685–11691.
[25] J. Miao, J. Sunarso, X. Duan, et al., J. Hazard. Mater. 349 (2018) 177–185.
[26] Y. Wang, D. Cao, X. Zhao, Chem. Eng. J. 328 (2017) 1112–1121.
[27] H. Lin, J. Wu, H. Zhang, Chem. Eng. J. 244 (2014) 514–521.
[28] S. Khan, X. He, J.A. Khan, et al., Chem. Eng. J. 318 (2017) 135–142.
[29] G. Liu, H. Lv, H. Sun, X. Zhou, Ind. Eng. Chem. Res. 57 (2018) 2396–2403.
[30] B. Qiu, L. Cai, Y. Wang, et al., Mater. Today Energy 11 (2019) 89–96.
[31] B. Qiu, C. Wang, N. Zhang, ACS Catal. 9 (2019) 6484–6490.
[32] B. Qiu, L. Cai, Y. Wang, et al., Small 15 (2019) 1904507.
[33] M. Xing, W. Xu, C. Dong, et al., Chem 4 (2018) 1359–1372.
[34] B. Sheng, F. Yang, Y. Wang, et al., Chem. Eng. J. 375 (2019) 121989.
[35] S. Wang, W. Xu, J. Wu, Q. Gong, P. Xie, Sep. Purif. Technol. 235 (2020) 116170.
[36] Y. Yao, Z. Yang, H. Sun, S. Wang, Ind. Eng. Chem. Res. 51 (2012) 14958–14965.
[37] X. Dong, B. Ren, Z. Sun, et al., Appl. Catal. B: Environ. 253 (2019) 206–217.
[38] L. Chen, X. Zuo, S. Yang, T. Cai, D. Ding, Chem. Eng. J. 359 (2019) 373–384.
[39] G. Peng, T. Li, B. Ai, et al., Chem. Eng. J. 360 (2019) 1119–1127.
[40] C. Tan, X. Lu, X. Cui, et al., Chem. Eng. J. 363 (2019) 318–328.
[41] S. Yang, X. Qiu, P. Jin, et al., Chem. Eng. J. 353 (2018) 329–339.
[42] J. Wang, L. Kou, L. Zhao, et al., Chemosphere 248 (2020) 126076.
[43] C. Cai, S. Kang, X. Xie, et al., J. Hazard. Mater. 385 (2020) 121519.
[44] H. Li, C. Shan, B. Pan, Environ. Sci. Technol. 52 (2018) 2197–2205.
[45] D. Ding, S. Yang, L. Chen, et al., Chem. Eng. J. 392 (2020) 123725.
[46] C. Tan, X. Jian, Y. Dong, et al., Chem. Eng. J. 359 (2019) 594–603.
[47] Z. Yang, Y. Li, X. Zhang, et al., Chem. Eng. J. 384 (2020) 123319.
[48] S. Zhu, Y. Xu, Z. Zhu, Z. Liu, W. Wang, Chem. Eng. J. 384 (2020) 123298.
[49] T. Zeng, H. Zhang, Z. He, J. Chen, S. Song, Sci. Rep. 6 (2016) 33348.
[50] Q. Yi, J. Tan, W. Liu, et al., Chem. Eng. J. 400 (2020) 125965.
[51] H. Nan, Z. Wang, W. Wang, et al., ACS Nano 8 (2014) 5738–5745.
[52] X. Huang, X. Zhou, J. Zhou, et al., Water Res. 122 (2017) 701–707.
[53] Y. Feng, P. Lee, D. Wu, K. Shih, Environ. Sci. Technol. 51 (2017) 2312–2320.
[54] X. Duan, Z. Ao, H. Sun, et al., Chem. Commun. 51 (2015) 15249–15252.